

Potential Fluctuation Associated with Energetic-Particle Induced Geodesic Acoustic Mode in Reversed Magnetic Shear Plasmas on LHD

T. Ido 1)2), A. Shimizu 1), M. Nishiura 1), S. Nakamura 1), S. Kato 1), H. Nakano 1), Y. Yoshimura 1), K. Toi 1)2), K. Ida 1), M. Yoshinuma 1), S. Satake 1), F. Watanabe 3), K. Itoh 1), S. Kubo 1)2), T. Shimozuma 1), H. Igami 1), H. Takahashi 1), I. Yamada 1), K. Narihara 1) and the LHD experiment group

- 1) National Institute for Fusion Science, Oroshi-cho, Toki-shi, Gifu, 509-5292, Japan
- 2) Nagoya University, Nagoya 464-8603, Japan
- 3) Kyoto University, Kyoto 606-8502, Japan

E-mail contact of main author: ido@LHD.nifs.ac.jp

Abstract. Geodesic acoustic mode(GAM) driven by energetic particles are observed in the Large Helical Device by a heavy ion beam probe. The GAM frequency shifts upward in plasmas with monotonic magnetic shear. In plasmas with reversed magnetic shear, on the other hand, the observed GAM and the energetic-particle induced mode, which is probably reversed-shear induced Alfvén Eigenmode(RSAE), appears, and the GAM frequency becomes constant. The GAM in the reversed-shear plasma localizes near the magnetic axis. It is confirmed that the energetic-particle induced GAM is accompanied by the electrostatic potential fluctuation and the radial electric field fluctuation. The amplitude of the potential fluctuation is several hundred volts, and it is much larger than the potential fluctuation associated with turbulence-induced GAMs observed in the edge region in tokamak plasmas. The energetic-particle induced GAM modulates the amplitude of the ambient density fluctuation at the GAM frequency.

1. Introduction

Energetic-particle driven Alfvén eigenmode(AE) is concerned to enhance the radial transport of energetic particles, such as alpha particles in the D-T reaction, and to deteriorate the performance of fusion reactors. Therefore, the study of the energetic-particle driven modes is a crucial issue in fusion research and investigated using various methods[1]. Recent works[2-6] indicate that the energetic particles drive geodesic acoustic mode (GAM) as well as AEs. The GAM[7] also attracts much attention as a branch of turbulence-driven zonal flows in the area of turbulent-transport study[8-10], because the excitation of the zonal flow by the nonlinear coupling of turbulence results in the reduction of the energy of the turbulence and turbulent transport and the sheared flow of the zonal flow affect the behaviours of the turbulence. Hitherto, the turbulence-induced zonal flow has been studied mainly based on the flow or radial electric field(E_r) measurement, because the flow and E_r , which drives a flow is essential in the phenomena. The direct and simultaneous measurement of zonal flow and ambient turbulence reveals not only the characteristics of the zonal flow itself but also the interaction between the zonal flow and turbulence[11-14]. On the other hand, the E_r fluctuation associated with the energetic-particle driven GAM (EGAM) have not been measured, except for a large potential fluctuation reported in Ref.[15]. In this work, the electrostatic potential fluctuation associated with the EGAM are measured directly by a heavy ion beam probe(HIBP) in the Large Helical Device(LHD), and the characteristics are presented.

2. Apparatus

LHD[16] is a superconducting heliotron device with a major radius of 3.9 m and an averaged minor radius of 0.65 m, and its magnetic field strength on the magnetic axis is up to about 3 T.

In order to measure the electrostatic potential in the LHD plasma, an HIBP using a 6-MeV gold ion beam is installed[17]. The temporal resolution is about 500 kHz, the spatial resolution is estimated to be a few cm[18]. The resolution of the potential measurement is experimentally confirmed up to $\Delta\phi/E_b = 1.6 \times 10^{-5}$, where ϕ and E_b is the electrostatic potential at the measurement position and the beam energy, respectively. Since $E_b = 1.375$ MeV in this experiment, it is ensured that $\Delta\phi \sim 22$ V. The electrostatic potential profile can be measured along the curve in Fig.1 by scanning the probe beam. The scanning frequency is 10 Hz.

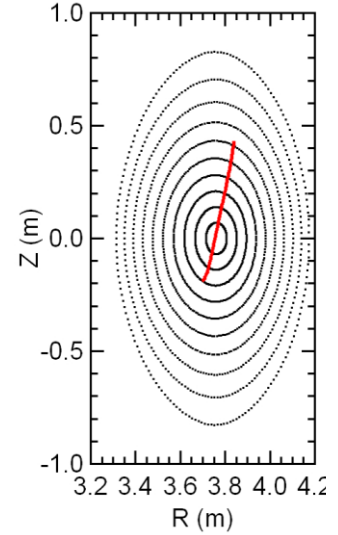


FIG.1 Observable region during the scanning a probing beam.

3. Experimental results

3.1. Experimental condition

A typical discharge pattern is shown in Fig.2 (a) and (b). The major radius of the magnetic axis is 3.75 m, the effective minor radius of the magnetic surface in which 99 % of the stored energy is included (a_{99}) is 0.63 m, and the toroidal magnetic field strength is 1.5 T at the magnetic axis. The plasmas are produced and sustained by tangential neutral beam injections (NBIs) from 0.5 s to 2.5 s. 170 keV hydrogen beams are injected in co- and counter-direction, where the co-injection means that the beam-driven plasma current increases the original rotational transform. The power of NBIs is balanced so as to minimize the beam-driven plasma current. The total absorbed power is 4.3 MW. The line averaged electron density is $0.1 \times 10^{19} \text{ (m}^{-3}\text{)}$ and almost constant during the discharges. In the discharges, fuel gas is not injected so as to keep the density low, and impurity (carbon) ions are

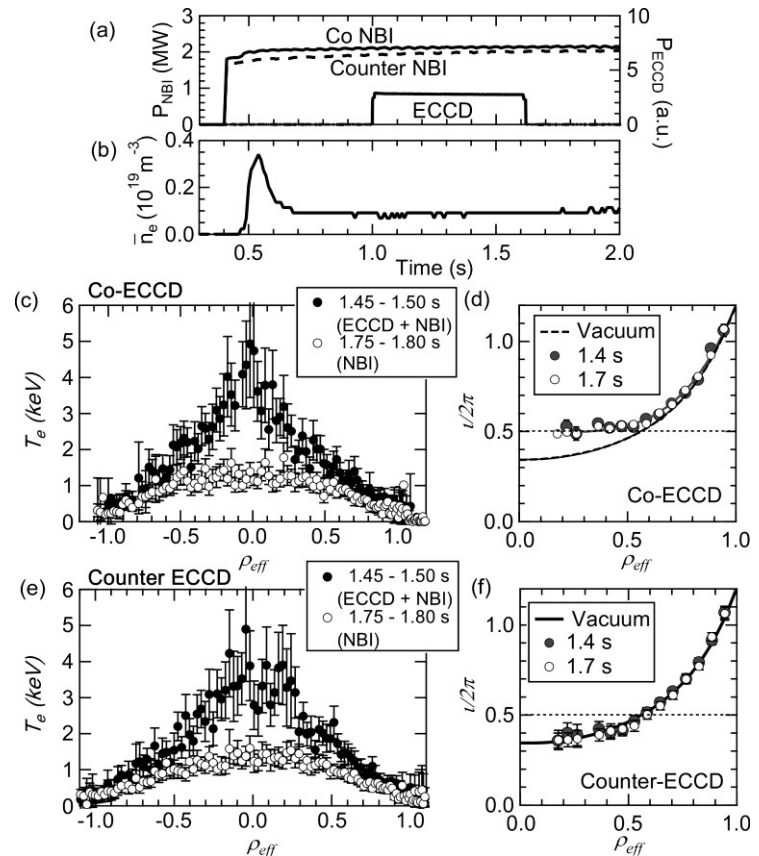


FIG.2 (a) Timing of NBI and ECCD. (d) Line averaged electron density. (c) and (e): Electron temperature profiles. The horizontal axis is an averaged minor radius normalized by effective minor radius the plasma (0.63 m). (d) and (f): Rotational transform profiles. ECCD is superposed from 1.0 s to 1.6 s. In (c) and (d), ECCD is co-direction, and in (e) and (f) ECCD is counter-direction.

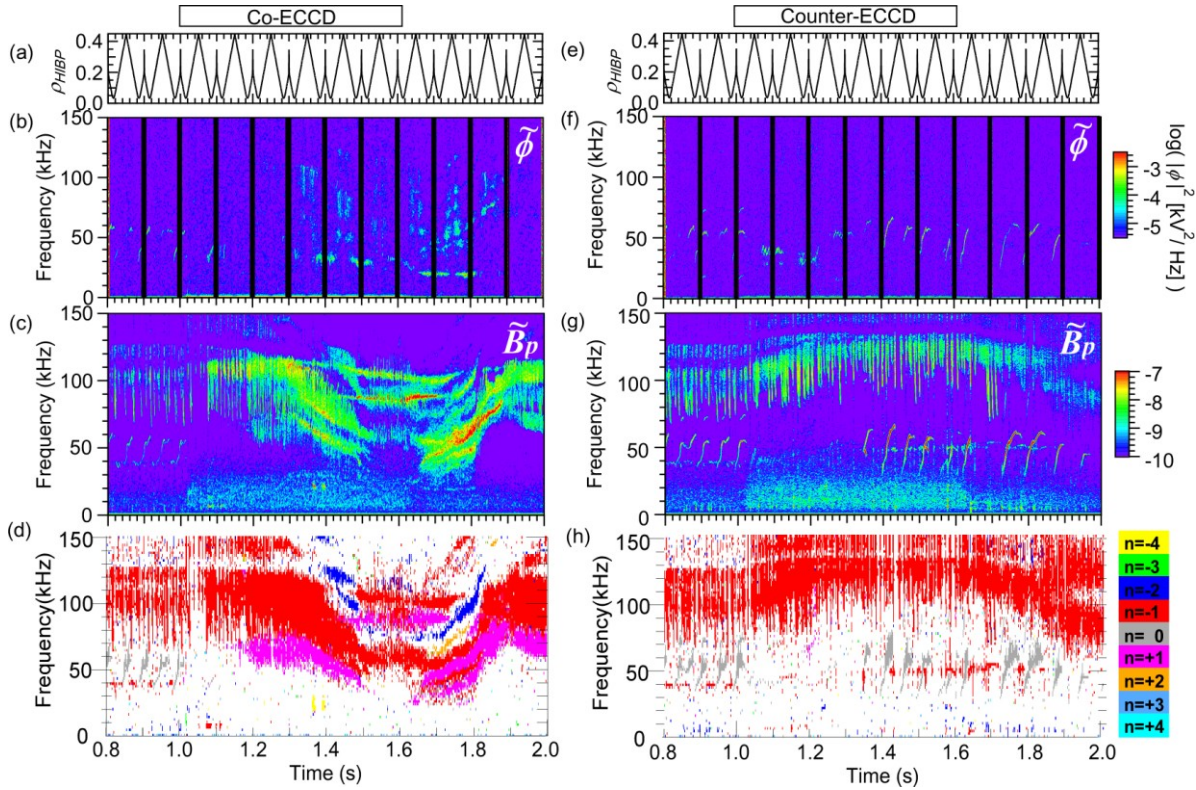


FIG.3. (a) and (e): Measurement position of the HIBP. (b) and (f): Spectrograms of the electrostatic potential fluctuation measured by the HIBP. (c) and (g): Spectrograms of the magnetic field fluctuation measured by a Mirnov coil. (d) and (h): toroidal mode estimated using toroidal magnetic probe (Mirnov coil) array. The left and right hand figures show the temporal behaviours in discharges with co-ECCD (weak or reversed magnetic shear) and counter-ECCD (strong magnetic shear), respectively.

dominant in the bulk ions in such low density plasmas as shown by the visible Bremsstrahlung measurement [19].

The electron cyclotron current drive (ECCD) with the power of 300 kW is superposed from 1.0 s to 1.6 s. The direction of the current drive can be changed shot by shot.

The temperature profiles measured by the Thomson scattering and the rotational transform profiles measured by the motional Stark effect spectroscopy (MSE) are shown in Fig.2. During the ECCD in the co-direction, the rotational transform increases near the central region and that weak or reversed magnetic shear profiles are formed [20].

3.2. Characteristics of the GAM

Spectrograms of the potential fluctuation measured by the HIBP and the poloidal magnetic field fluctuation measured by a Mirnov coil are shown in Fig.3. Note that the spectrogram of the potential fluctuation (Fig.3 (b) and (f)) includes spatial information as well as temporal evolution because the measurement position of the HIBP is scanned between $r_{eff}/a_{99} (\equiv \rho_{eff}) = 0.1$ and 0.4 at the frequency of 10 Hz (Fig. 3(a) and (e)), where r_{eff} is averaged minor radius. Several modes are observed in the spectrograms. Since they are not observed in other plasmas without the tangential NBI, they are induced by energetic particles from the tangential NBIs.

Before the start of the superposition of ECCD (0.8 – 1.0 s), upward shift of the frequency with the time constant of about 10 ms is observed in the frequency range between 30 and 60 kHz in the electrostatic potential fluctuation (Fig.3 (b) and (f)) and the magnetic fluctuation (Fig.3 (c) and (g)). Since the toroidal mode number is zero (as shown in gray in Fig.3 (d) and (h)) and the initial frequency is in the same range as the predicted GAM frequency (~ 30 kHz), the mode is probably the energetic-particle driven GAM [3, 4].

After the start of ECCD in the co-direction at 1.0 s, the frequencies of several modes decrease gradually from 200 kHz to about 50 kHz with the time constant of a few hundred milliseconds (Fig.3 (b) and (c)). The toroidal mode number (n) estimated with the magnetic probe (Mirnov coil) array is one (Fig.3 (d)). Since the time constant reflects the change in the rotational transform profile and the change in the frequency is consistent with the temporal evolution of the shear Alfvén spectra [21], a candidate for the modes is reversed-shear induced Alfvén eigenmodes (RSAE) [22-24, 6].

In addition to that, a fluctuation with constant frequency of 32 kHz from 1.35 to 1.6 s (during ECCD) and 20 kHz from 1.65 to 1.8 s (after the termination of ECCD) is observed in the spectrogram of the electrostatic potential (Fig.3 (c)). The GAM frequency in helical systems is expressed [25] as

$$f_{GAM} = \frac{1}{2\pi R_0} \sqrt{\frac{T_e + \frac{7}{4}T_i}{M}} G,$$

where R_0 is the major radius of the magnetic axis, M is the ion mass, and T_i and T_e is the ion and electron temperatures respectively. G is a factor including the magnetic ripple, and it can be calculated analytically and numerically using a global Monte Carlo transport simulation code FORTEC-3D [26]. The calculated GAM frequencies are 37 ± 9 kHz during ECCD and 26 ± 8 kHz after the ECCD, and the observed frequencies roughly agree with them. The temperature dependence is shown in Fig.4, where the ion temperature

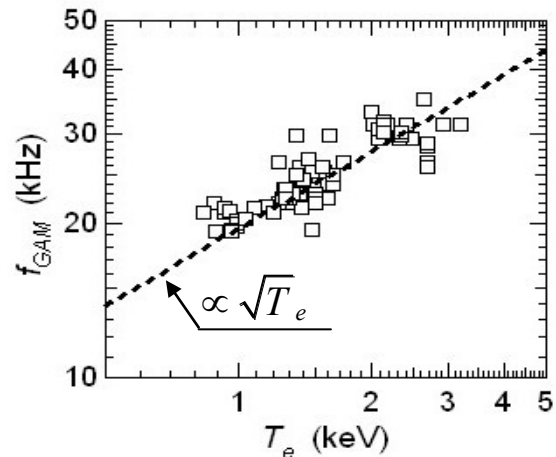


FIG.4. Temperature dependence of the observed GAM frequency.

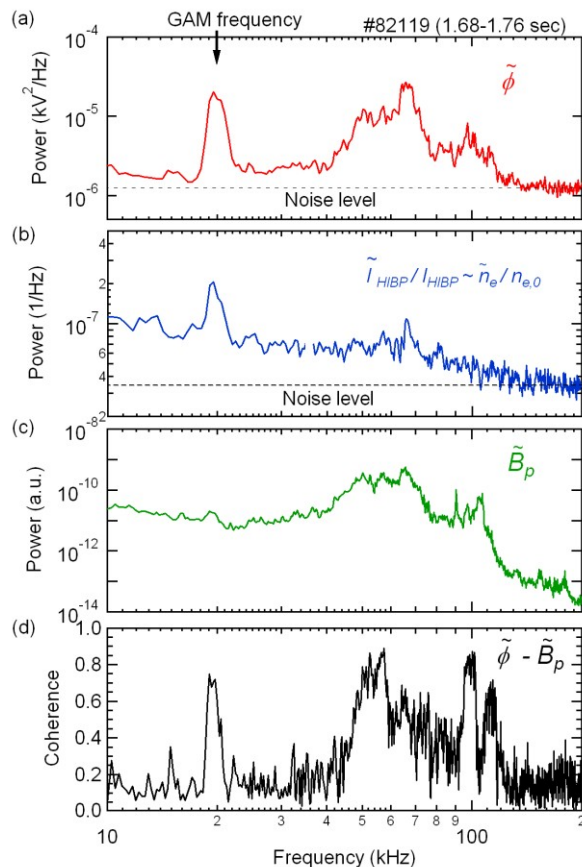


FIG.5 Frequency spectra of (a) electrostatic potential, (b) normalized-beam intensity which corresponds to the normalized-density fluctuation, and (c) magnetic field fluctuation. (d) Coherence between the electrostatic potential and magnetic field fluctuations. The observation position of the HIBP is at $r_{eff}/a_{99} \sim 0.15$.

is much lower than the electron temperature. The observed frequency is proportional to the square-root of the electron temperature, and the dependence is same as that of the GAM.

Figures 5 (a) - (c) show frequency spectra of the electrostatic potential fluctuation, the normalized intensity of the HIBP which reflects the normalized plasma density fluctuation, and the magnetic field fluctuation just after ECCD, respectively. The measurement position of the HIBP is at $\rho_{eff} \sim 0.15$. The mode with a frequency of 20 kHz is observed in the spectra of the electrostatic potential and density fluctuations. The magnetic field fluctuation is small at 20 kHz, however a significant coherence between the electrostatic potential fluctuation and magnetic field fluctuation in Fig.5 (d) indicates the mode is also accompanied by the magnetic field fluctuation. The toroidal mode number estimated using the toroidal magnetic probe array is zero[21]. The frequency and mode structure indicate that the mode is the GAM. Since the GAM has not observed in plasmas without the tangential NBI, the GAM is probably the energetic-particle driven GAM (EGAM).

In the case of counter-ECCD, the GAM with the constant frequency does not appear and the upward-shift of the frequency is repeated. According to ref.[2], the rapid frequency shift is caused by the creation of hole-clump[27] in the velocity space distribution of the energetic particle. In the plasmas with the reversed magnetic shear, energetic particle driven modes, which are probably RSAEs, are excited near the local minimum point of the rotational transform profile, and the GAM exists near the modes as shown later. The transport of the energetic particle by the RSAEs may disturb the creation of hole-clump and result in no shift of the GAM frequency.

3.2. The electrostatic potential fluctuation associated with the GAM

The temporal behaviour of the potential fluctuation associated with the GAM is shown in Fig.6. The experimental condition is same as that in the left figures in Fig.3; the GAM with constant frequency(~ 20 kHz) in the reversed magnetic field is discussed. The measurement position of the HIBP is at $\rho_{eff} \sim 0.1$. The amplitude of the potential fluctuation associated with the GAM is not constant. The root-mean-square of the amplitude is about

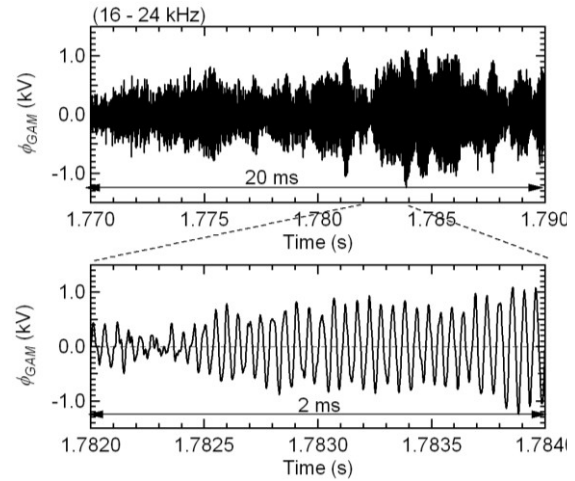


FIG.6. The temporal behaviour of the electrostatic potential fluctuation associated with the GAM, where the potential signal in the frequency range from 16 to 24 kHz is extracted using numerical filters. The experimental condition is same as that in the left figures in Fig.3

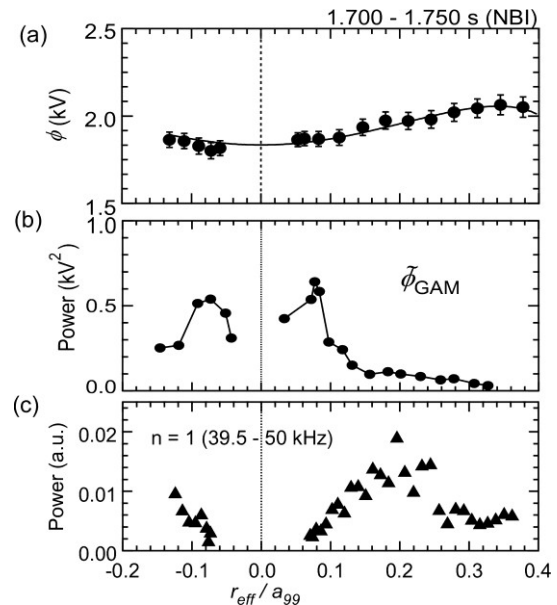


FIG.7. (a) Averaged electrostatic potential profile. (b) and (c) Power of potential fluctuations associated with the GAM and $n = 1$ mode, respectively. The analyzed data are obtained from 1.7 to 1.8 s in the discharge shown in the left figure in Fig.3.

500 V, and the maximum value reaches about 1 kV. The amplitude of the GAM is much larger than that of turbulence-induced GAM observed in the edge region in tokamak plasmas (cf. ~ 15 V in the edge plasma in JFT-2M tokamak[12]).

The spatial distribution of the fluctuations can be measured by scanning the probing beam of the HIBP during a discharge. Figure 7(a), (b) and (c) show the averaged potential profile and the radial profiles of the power of the potential fluctuations associated with the GAM and $n = 1$ mode observed in the left figures in Fig.3. The power of the GAM is obtained through averaging two profiles measured between 1.7 and 1.8 s. The GAM exists near the magnetic axis, and the $n = 1$ mode locates outside the GAM.

Since the GAM is accompanied by the magnetic fluctuation, the displacement of the magnetic surface(ξ) may induce the potential fluctuation at a measurement position: $\delta\phi(r) = E_r(r)\xi$. Figure 7 indicates that $\xi \leq 0.15$ which corresponds to $r_{eff} \sim 0.1$ (m) and $E_r < 1000$ (V/m). Thus, the measured potential fluctuation associated with the GAM is not attributed to the radial displacement of the magnetic surface. Therefore, it is confirmed that the observed GAM is accompanied by the electrostatic potential fluctuation. In addition to that, the gradient of the amplitude profile of the electrostatic potential fluctuation indicate that the GAM is accompanied by the radial field fluctuation.

It is expected that the flow induced by radial electric field fluctuation associated with the energetic-particle induced GAM affects ambient turbulence in the high frequency range because the modulation of the high frequency ambient turbulence by the turbulence-induced GAM is observed in the edge region in tokamak plasmas[11-14]. Since the electrostatic potential fluctuation associated with the GAM and the density fluctuation including the ambient turbulence are measured by the HIBP at the same position simultaneously, the relation between them is examined.

The ambient density fluctuation is extracted using a numerical high-pass-filter with the cut-off frequency of 120 kHz which is selected to be higher than the frequencies of the GAM(~ 20 kHz) and Alfvén Eigenmode(~ 60 kHz). Figure 8 (a) and (b) show the power spectra of the normalized density fluctuation and the extracted high-frequency ambient density fluctuation at $\rho_{eff} \sim 0.1$, respectively. The GAM and AE fluctuations which appear in the raw signal (Fig.8(a)) are removed from the extracted ambient density fluctuation signal as shown in Fig. 8 (b).

The power spectrum of the envelope of the high-frequency ambient fluctuation is shown in Fig. 8 (c), where the envelope is estimated using the Hilbert transform and it indicates the temporal evolution of the

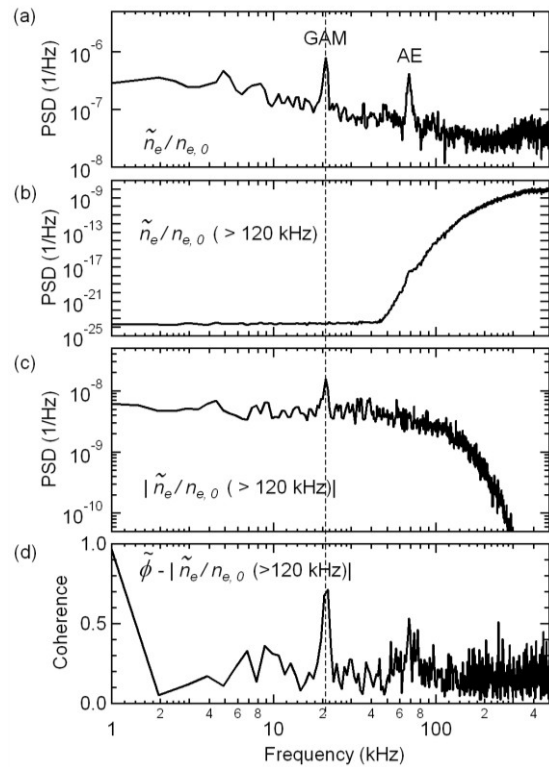


FIG.8. (a) Power spectrum of normalized density fluctuation measured by the HIBP. The experimental condition is similar to that at 1.7 s in the left figures in Fig.3, and the measurement position is at $\rho_{eff} \sim 0.1$. (b) Power spectrum of the high-frequency density fluctuation (ambient turbulence) which is extracted using a numerical high-pass-filter with the cut-off frequency of 120 kHz. (c) Power spectrum of the envelope of the ambient turbulence. (d) Coherence between the electrostatic potential fluctuation and the envelope of the ambient turbulence.

fluctuation amplitude. In Fig. 8 (c), a peak is observed at the GAM frequency, and it indicates that the amplitude of the ambient turbulence is modulated at the GAM frequency. Significant coherence between the electrostatic potential fluctuation and the envelope of the ambient density fluctuation is also observed at the GAM frequency in Fig. 8 (d). The results indicate that the ambient turbulence is modulated by the energetic-particle induced GAM. One of the candidates of the modulation is the distortion of the frequency spectrum by the Doppler shift owing to the flow associated with the GAM, and the other is the dynamic shearing of ambient turbulence by the GAM[28]. At present, the mechanism of the modulation is not concluded, because the poloidal wave number of the ambient turbulence and the absolute value of the radial electric field fluctuation are not measured. The influence on the turbulent transport by the energetic-particle induced GAM is a future issue.

4. Summary

The GAM induced by the energetic particles is observed directly and locally by the HIBP in LHD. The observed GAM frequency shifts upward in the monotonic magnetic shear plasmas. On the other hands, it becomes constant in the reversed magnetic shear plasmas.

The GAM in the reversed magnetic shear plasmas localizes near the magnetic axis, and it is accompanied by the electrostatic potential fluctuation, which is not caused by the magnetic surface fluctuation. The root-mean-square and maximum values of the amplitude are several hundred volts and about 1 kV, respectively. They are much larger than that of turbulence-driven GAM observed in edge region in tokamak plasmas. The simultaneous measurement of the electrostatic potential fluctuation and the density fluctuation reveals that the energetic-particle induced GAM affects the temporal behavior of the ambient turbulence in the high frequency range.

Acknowledgements

We appreciate Prof. Y. Todo, Prof. Emeritus T. Watari, Prof. Emeritus Y. Hamada of NIFS, and Prof. A. Fujisawa of Kyushu Univ., Dr. A. Melnikov of Kurchatov Institute, Prof. V.P. Shevelko of P.N. Lebedev Physical Institute, Prof. M. Wada of Doshisha Univ., and Dr. A. Taniike of Kobe Univ. for valuable discussion. We thank the LHD technical group for its support.

This work was supported by MEXT Japan under Grant-in-Aid for Young Scientists (Nos. 18760640 and 20686062), and NIFS/NINS under the project of Formation of International Network for Scientific Collaborations, NIFS09ULBB505 and NIFS09ULBB515.

Reference

- [1] HEIDBRINK, W., "Basic physics of Alfvén instabilities driven by energetic particles in toroidally confined plasmas", *Phys. Plasmas* **15** (2008) 055501.
- [2] BERK, H. et al., "Explanation of the JET n= 0 chirping mode", *Nucl. Fusion* **46** (2006) S888.
- [3] NAZIKIAN, R. et al., "Intense geodesic acousticlike modes driven by suprathermal ions in a tokamak plasma", *Phys. Rev. Lett.* **101** (2008) 185001.
- [4] FU, G., "Energetic-Particle-Induced Geodesic Acoustic Mode", *Phys. Rev. Lett.* **101** (2008) 185002.
- [5] ZONCA, F. et al., "Kinetic theory of Geodesic Acoustic Modes: radial structures and nonlinear excitations", *Proc. 22nd Int. Fusion Energy Conf. 2008* (Geneva, Switzerland, 2008) (2008).

- [6] TOI, K. et al., “Observation of Reversed Shear Alfvén Eigenmode Excited by Energetic Ions in a Helical Plasma”, *Phys. Rev. Lett.* (2010).
- [7] WINSOR, N. et al., “Geodesic Acoustic Waves in Hydromagnetic Systems”, *Phys. Fluids* **11** (1968) 2448.
- [8] DIAMOND, P. H. et al., “Review of zonal flows”, *Plasma Phys. Control. Fusion* **47** (2005) R35.
- [9] ITOH, K. et al., “Physics of zonal flows”, *Phys. Plasmas* **13** (2006) 055502.
- [10] FUJISAWA, A. et al., “Experimental progress on zonal flow physics in toroidal plasmas”, *Nucl. Fusion* **47** (2007) S718.
- [11] MCKEE, G. et al., “Experimental characterization of coherent, radially-sheared zonal flows in the DIII-D tokamak”, *Phys. Plasmas* **10** (2003) 1712.
- [12] IDO, T. et al., “Geodesic-acoustic-mode in JFT-2M tokamak plasmas”, *Plasma Phys. Control. Fusion* **48** (2006) S41.
- [13] NAGASHIMA, Y. et al., “In search of zonal flows by using direct density fluctuation measurements”, *Plasma Phys. Control. Fusion* **49** (2007) 1611.
- [14] LAN, T. et al., “Spectral features of the geodesic acoustic mode and its interaction with turbulence in a tokamak plasma”, *Phys. Plasmas* **15** (2008) 056105.
- [15] TOI, K. et al., “Alfvén Eigenmodes and Geodesic Acoustic Modes Driven by Energetic Ions in an LHD Plasma with Non-monotonic Rotational Transform Profile”, in *22nd IAEA Fusion Energy Conference, Geneva, EX_P8-4*, 2008.
- [16] IIYOSHI, A. et al., “Overview of the large helical device project”, *Nucl. Fusion* **39** (1999) 1245.
- [17] IDO, T. et al., “Development of 6-MeV Heavy Ion Beam Probe on LHD”, *Fusion Sci. Tech.* **58** (2010) 436.
- [18] IDO, T. et al., “Measurement of electrostatic potential fluctuation using heavy ion beam probe in large helical device”, *Rev. Sci. Instrum.* **79** (2008) 10F318.
- [19] ZHOU, H. et al., “Investigation on Total Bremsstrahlung Radiation in High-Density Operation of LHD Based on Visible Bremsstrahlung Profile Measurement”, submitted to *Japanese Journal of Appl. Phys.* (2010).
- [20] KUBO, S. et al., “Profile control by local ECRH in LHD”, in *22nd IAEA Fusion Energy Conference, Geneva, 2008, EX_P6-14*, 2008.
- [21] IDO, T. et al., “Experimental study of radial electric field formation and electrostatic potential fluctuation in the Large Helical Device”, in *37th EPS Conference on Plasma Physics (submitted to Plasma Phys. Control. Fusion)*, 2010.
- [22] KIMURA, H. et al., “Alfvén eigenmode and energetic particle research in JT-60 U”, *Nucl. Fusion* **38** (1998) 1303.
- [23] SHARAPOV, S. et al., “Alfvén wave cascades in a tokamak”, *Phys. Plasmas* **9** (2002) 2027.
- [24] FUKUYAMA, A. et al., “Kinetic Global Analysis of Alfvén Eigenmodes in Toroidal Plasmas”, in *19th IAEA Fusion Energy Conference, Lyon, France, TH_P3-14*, 2002.
- [25] SUGAMA, H. et al., “Collisionless damping of zonal flows in helical systems”, *Phys. Plasmas* **13** (2006) 012501.
- [26] SATAKE, S. et al., “Non-local neoclassical transport simulation of geodesic acoustic mode”, *Nucl. Fusion* **45** (2005) 1362.
- [27] BERK, H. et al., “Spontaneous hole-clump pair creation in weakly unstable plasmas”, *Phys. Lett. A* **234** (1997) 213.
- [28] ITOH, K. et al., “Excitation of Geodesic Acoustic Mode in Toroidal Plasmas”, *Plasma Phys. Controlled Fusion* **47** (2005) 451.